Journal of Advanced Manufacturing and Processing

WILEY | AIChE The Global Home of Chemical Engineers

RESEARCH ARTICLE OPEN ACCESS

Polypropylene Composites Reinforced With Recycled Waste Cellulosic Fiber/Fine Mixture: The Impact of Cellulose Sieving on Performance

Emmanuel Akubueze | Atul Kumar Maurya | Patrick Masembe | Niyi G. Olaiya | Nicholas Bowen | Davide Masato | Margaret J. Sobkowicz | Amir Ameli

Department of Plastics Engineering, University of Massachusetts Lowell, Lowell, Massachusetts, USA

Correspondence: Amir Ameli (amir_ameli@uml.edu)

Received: 5 August 2024 | **Revised:** 3 June 2025 | **Accepted:** 11 June 2025

Funding: This work was supported by U.S. Department of Energy, DE-EE0007897.

Keywords: composite | mechanical properties | natural fiber | polypropylene | reinforcement | sieving | waste cellulose

ABSTRACT

This study explores how a sieving step of waste cellulosic fiber and fine (WCFF) mixture affects the performance of WCFF-loaded polypropylene (PP) composites and whether the separation of fines from fibers offers an added benefit. The WCFF samples were downsized, and four different filler size ranges were sieved using a series of mesh sizes from 4 to 0.85 mm. The WCFF/PP composites were then compounded at 20 wt.% loading of WCFF using a twin-screw extruder. Incorporating WCFF increased the tensile strength to 41.28 MPa and the modulus to 3207 MPa, accounting for 28% and 38% enhancements, respectively. Interestingly, the greatest improvements were associated with the nonsieved WCFF case, and the sieved WCFF fibers provided only marginal enhancements over virgin PP. The outperformance of nonsieved WCFF was attributed to the synergistic reinforcement of hybrid fibers and fines as well as the maintenance of longer fibers in the system. However, the strain at break and impact strength of PP decreased after introducing WCFF. Moreover, the complex viscosity and storage modulus increased with an increase in the filler size, due to the formation of a more effective percolative network. The PP's crystallinity exhibited a relatively strong dependency on the sieving, where WCFF samples with short-aspect-ratio fillers promoted the crystallinity significantly. It was also found that the WCFF degradation onset temperature increased once it was incorporated into PP. This study suggests that waste cellulosic feedstocks can be utilized as a reinforcement without additional sieving to manufacture high-performance and cost-effective composites.

1 | Introduction, Motivation, and State-of-the-Art

The reusability of any material including bio-based reinforcing agents significantly impacts cost reduction and less energy consumption, compared to their pristine counterparts [1, 2]. To this end, industrial wastes such as fly ash, pineapple crown fibers, crumb rubber, walnut shell powder, and recycled newspaper have been introduced to polymeric systems to prepare polymer composites [3–6]. One significant source of cellulose-based reinforcement is paper mills waste, which is a mixture of fibers and fines. Currently, the waste cellulosic fiber and fine (WCFF) mixture is not recycled and is either landfilled or burned. Without proper recycling measures, WCFF represents a missed opportunity for resource recovery and sustainable material utilization. These materials can potentially find applications in various industries, thereby reducing the demand for virgin resources and minimizing environmental impacts. By recycling WCFF, its inherent value as a source of cellulose material can be harnessed to produce bio-composites, insulation materials, paper products, and more. Moreover, recycling WCFF aligns with the principles

of the circular economy, where resources are kept in use for as long as possible, and waste is minimized through efficient resource management.

Among various potential applications, the utilization of WCFF towards developing natural fiber reinforced polymer composites seems promising, as such composites have been well developed using pristine natural fibers. However, the presence of hydrophilic groups such as —OH in cellulose makes them less compatible with hydrophobic polymers such as polypropylene (PP) and polyethylene (PE). It has been reported that the lack of interfacial interactions between reinforcing fiber and polymer matrix results in inferior mechanical properties of the composite. To address this issue, various compatibilization techniques, such as surface treatment of fiber and the use of a coupling agent, have been reported. Recently, Maurya et al. [7] presented a review of industrially relevant natural fiber reinforced PP hybrid composites, considering sisal, flax, kenaf, hemp, and coir fibers. Overall, they found that chemical treatment is preferred over physical treatment, as mechanical interlocking is the only load transfer mechanism in the latter case. Furthermore, chemical treatment (e.g., silane, alkali-silane, alkaline, acetylation) tailors the fiber surface and enhances the compatibilization at the interface of natural fiber and polymeric matrix. Alkali treatment is the most employed technique for the chemical treatment of natural fibers for composite fabrication [8]. For instance, El-Abbassi et al. [9] soaked the alfa fiber in salt water (35 g/L) for 24 h at 60°C, followed by 10% NaOH treatment. The authors reported an improvement of 18% in the tensile strength for 30 wt.% fiber-reinforced PP composites. Similar to chemical treatment, compatibilization is another promising route that has been extensively used to enhance the interaction between surfaces of natural fibers and polymeric matrices [7]. Lu et al. [10] stated that any material that reduces the interfacial energy between the two separate phases or enhances the dispersion of fibers within the matrix can be termed as a compatibilizer. Monofunctional isocyanates and maleic anhydride grafted PP (MA-g-PP) are common compatibilizers. MA-g-PP promotes esterification and/or hydrogen bonds between the —OH groups of fiber and the -MA groups of MA-g-PP. Chain entanglement between MA-g-PP and PP is also exhibited during compatibilization due to the incorporation of MA-g-PP in the natural fiber and polymer composite system [7]. In other studies, MA-g-PP [11], MA-g-styrene-ethylene-butylene-styrene (SEBS) [12] and MA-g-ethylene-propylene rubber (EPR) [4] have also been reported as compatibilizers for the fabrication of PP composites reinforced with bamboo fiber, sisal fiber, and pineapple leaves, respectively. All these composites demonstrated improved tensile strength and modulus by incorporating compatibilizer. Moreover, using compatibilizers instead of chemical or physical treatment of the fibers saves significant effort, energy, and cost. On an industrial scale, using a compatibilizer would also be an easier step compared to fiber treatments. Although most reports on natural fiber reinforced polymer composites focus on the analysis of the mechanical performance, rheological analysis upon incorporation of fibers and compatibilizers is also important. It can serve dual purposes—optimizing the melt processing of the composites and evaluating the microstructure of the composites (e.g., dispersion quality and percolation) [13]. Solid reinforcements significantly hinder polymer chain mobility in the melt state, which in turn is influenced by dispersion, shape and surface modification, and particle size of the reinforcement [13, 14].

However, limited work has been reported on using industrial paper mill waste as a potential reinforcing agent in PP composites. This waste usually contains both large aspect ratio fibers as well as fines that resemble zero dimensional particles (i.e., aspect ratio of about one). It is thus crucial to study the reinforcing role of these hybrid waste cellulosic materials and more importantly how the presence of the fines may affect the reinforcing capability. Therefore, this work explores the potential of WCFF towards high performance PP composites. The focus is on examining the effects of WCFF sieving and MA-g-PP compatibilizer on the mechanical, rheological, and thermal properties of the WCFF/PP composites.

2 | Materials and Methods

2.1 | Materials

The recycled waste cellulosic fibers and fines were supplied in pellet form by the American Wood Fibers (AWF), United States. PP, grade PRIMATOP^{R} PPC 05030 was procured from AMCO polymers. As per the manufacturer, it had a density, melt mass flow rate (MFR at 230°C/2.16 kg), and tensile yield strength of 0.90 cm^3/g, 5 g/10 min, and 33.44 MPa, respectively. Coupling agent MA-g-PP was obtained from SK functional polymers under the trade name Orevac-CA100. The coupling agent had a density and MFR of 0.91 g/cm^3 and 10 g/10 min, and a comparable price range to that of the PP.

2.2 | Fabrication Procedure

2.2.1 | WCFF Preprocessing

As received, WCFF pellets were subjected to mechanical grinding for 90 s in a high-speed blender. This mild grinding aimed to achieve optimal fiber dissociation to maintain a suitable bulk density for consistent feeding during subsequent processing while preventing significant fiber breakage. The grinded WCFF pellets were analyzed using a MorFi Analyzer (Pichincha, Ecuador) for their size distribution. Particles with an aspect ratio greater than unity were considered fibers, and those with an aspect ratio of one or less were termed fines. Fiber analysis showed that about 55 wt.% of WCFF was in fiber form (with an average aspect ratio of about 30) and the remaining 45 wt.% was fines. The grinded WCFF was then sieved to obtain three different size ranges. A stack of sieves with varying mesh sizes was used, with the largest openings at the top and smallest at the bottom. The samples were poured onto the top sieve, and a mechanical shaker was used to guide the samples through the sieves. The samples were collected in three mesh size ranges: 1.7–4 mm (SF1), 0.85–1.7 mm (SF2), and less than 0.85 mm (SF3) as given in Table 1. The WCFF batches then underwent a controlled two-step drying process (12 h at 80°C and 5 min at 120°C) using a conventional oven. This process ensured a final moisture content below 1 wt.%, as measured by a Computrac Vapor Pro XL (S/N: 42000272) Moisture Analyzer.

TABLE 1 | Sample codes and compositions of PP and WCFF/PP composites.

Sample code	PP (wt.%)	MA-g-PP (wt.%)	WCFF (wt.%)	WCFF mesh size
PP	100	0	0	—
PP+MA-g-PP	97	3	—	—
SF0-MA0	80	0	20	Not sieved
SF0	77	3	20	Not sieved
SF1	77	3	20	4 > WCFF > 1.7
SF2	77	3	20	1.7 > WCFF > 0.85
SF3	77	3	20	WCFF < 0.85

2.2.2 | Compounding of WCFF/PP Composites

Table 1 gives the sample code and the composition of the composites. MA-g-PP was used at an optimized content of 3 wt.% after screening experiments from 0 to 5 wt.% loading. WCFF was used at 20 wt.% loading, as an intermediate loading content to analyze the mesh size effect. Preliminary results showed that WCFF can be loaded up to 40 wt.%. Compounding of all the samples was performed using a twin-screw extruder (Leistrtiz ZSE 18HP) with a diameter of 18 mm and an L/D ratio of 40. PP and MA-g-PP were dry blended and fed together from a feeder, whereas WCFF were dosed and fed using another feeder. A total throughput of 50 g/min and a screw speed of 300 rpm were maintained for all the composite compositions. The extruder temperature was also kept at 180°C or below, and the extrudates were cooled down, passing through a water bath before pelletization. The pelletized compounds were dried in an air oven maintained at 80°C to remove moisture before further processing or testing.

The compounded pellets were then compression molded (CARVER INC. model 4394.4PL3003) into 0.62 mm flat sheets under a pressure of 103 MPa and a temperature of 180°C. The compression cycle lasted 8 min, followed by system-controlled water cooling to 20°C in 5 min to control the cooling rate and stabilize the molded sheets. Following a modified ASTM D638, type V tensile samples were die-cut from the sheets. Microscopy samples were made by cryo-fracturing a small sample cut from the same compression molded sheets. For rheology tests, circular discs of 25 mm in diameter and 2 mm in thickness were prepared from the compounded pellets using an Xplore IM12 micro injection molding machine at 200°C. For thermal analysis, pellets were used as compounded.

2.2.3 | Testing and Characterization

The fracture surface morphology of the cryo-fractured composites was characterized using a scanning electron microscope (SEM, Make: JEOL (JSM 6390)) at an acceleration voltage of 5 kV. Prior to SEM characterization, gold sputtering was provided for 3 min on all the samples using Vacuum Desk IV sputter coater.

Rheological properties were measured using an ARES G2 rheometer (TA Instruments, Series: 4010–0218) with 25 mm stainless steel parallel plates and a 1.5 mm gap. Tests were conducted in the linear viscoelastic region at 5% strain. Oscillation frequency sweeps (100–0.1 rad/s) at 170°C and 230°C were conducted. The samples' melt flow index (MFI) was also measured using a Dynisco IM 500 melt flow indexer in accordance with ASTM D1238. After loading about 10 g of material into the plastometer cylinder, it was heated up for 90 s at 200°C. The sample was then subjected to a 2.16 kg weight following the preheating process. The extrudate mass was measured every 1 min for five times to determine the average MFI value in g/10 min for each sample.

The tensile properties were tested as per ASTM D638 standard (type V) on Instron 5966 with a 10 kN load cell. A displacement rate of 10 mm/min was used, providing a nominal strain rate of 1 mm/(mm min) at the start of the test. At least 5 specimens of each sample were tested, and the average and standard deviation values of tensile strength, Young's modulus, and elongation at break are reported. The Izod impact test was performed according to ASTM D256. A rectangular bar measuring 64 × 12.7 × 3.2 mm was compression molded and a notch with a depth of 2.5 mm was created. The specimen was secured in the pendulum impact test fixture with the notched side directed towards the pendulum's striking edge. The pendulum was then released to strike the specimen. The average impact strength was measured from five samples for each composition.

Thermal properties, that is crystallinity, crystallization temperature, and melting point were measured using a differential scanning calorimetry (DSC, Mettler Toledo DSC 3+, C151224649). Both heating and cooling cycles were investigated as per ASTM D3418-15 standard. About 6 mg of each sample was placed in an aluminum pan and heated up to 250°C and maintained for 5 min to remove any thermal history. The samples were then cooled down to −50°C. After cooling, the samples were heated up again to 250°C to obtain the second heating thermograms. The crystallinity of PP was calculated using:

$$X_c(\%) = \frac{\Delta H_m}{\Delta H_m^{\circ} \cdot w_{PP}} \times 100 \quad (1)$$

where, ΔH_m is the melting enthalpy of the tested sample, ΔH_m° is the melting enthalpy of 100% crystalline PP (207 J/g), and w_{pp} is the weight fraction of PP in the composite. Moreover, to study thermal stability and degradation behavior, thermogravimetric analysis (TGA) was performed using Mettler Toledo TGA

2: CIS1224647 from 50°C to 600°C at 20°C/min heating ramp under a nitrogen environment.

3 | Results and Discussion

3.1 | The Role of MA-g-PP

Figure 1 shows the SEM micrographs of WCFF/PP composites without MA-g-PP and with 3 wt.% MA-g-PP. The comparison of the two SEM micrographs clearly shows the effect of MA-g-PP. In the case of no MA-g-PP (Figure 1a), fiber pullouts and the separation of fibers from the matrix at the interface are visible. However, once 3 wt.% MA-g-PP is added (Figure 1b), the morphology changes significantly; no fiber pullouts are visible, and the interfaces appear to remain more intact. Moreover, the addition of 3 wt.% of MA-g-PP to the composite system led to a better state of dispersion and distribution of the WCFF. As seen in Figure 1a, the composite without MA-g-PP had a rougher surface, which could be attributed to significant agglomeration of the cellulose fines/fibers, as opposed to Figure 1b, where the surface is smoother, due to a more uniform dispersion of WCFF at the presence of MA-g-PP. These observations are in line with the report by Kim et al. [15], where the authors fabricated natural fiber-reinforced PP composites with and without compatibilizer and showed that the composites with compatibilizers exhibited enhanced interfacial interactions.

Figure 2 shows the stress–strain curves as well as the tensile strength and modulus of PP and PP+MA-g-PP samples. Both PP and PP+MA-g-PP exhibited ductile behavior with yielding, as expected. With the incorporation of 3 wt.% MA-g-PP, a decrease in both tensile strength and modulus of PP was observed, whereas its elongation at break did not vary significantly. The pristine PP exhibited a tensile strength, modulus, and elongation at break of 32.45 MPa, 2329 MPa, and 330%, respectively, whereas these values for PP+MA-g-PP sample were 29.48 MPa, 2176 MPa, and 331%, corresponding to 9.1% and 6.6% decreases in strength and modulus, respectively. The decrease in tensile properties due to the incorporation of MA-g-PP might be attributable to the lower tensile properties of the MA-g-PP compared to pristine PP [16]. Likewise, Figure 2c,d show the stress–strain curve as well as the tensile strength and modulus of WCFF/PP composites, respectively. Samples SF0 and SF0-MA0 are WCFF/PP composites with and without MA-g-PP (Table 1). SF0 exhibited a tensile strength of 41.29 MPa while that for SF0-MA0 was 36.59 MPa, accounting for about 12.9% difference. Likewise, the composites with and without MA-g-PP demonstrated a tensile modulus of 3207 and 2957 MPa, respectively, demonstrating an 8.5% difference. The increase in the tensile strength and modulus of WCFF/PP composite with the addition of MA-g-PP is attributed to a better dispersion of fibers and fines as well as the enhanced interfacial bonding enabled by the interactions between the WCFF and MA groups of MA-g-PP. It has been reported in the literature that the hydroxyl group of the natural fiber interacts with the maleic anhydride and makes strong ester linkage at the interface of the fiber and the polymer matrix [10], which promotes a more effective load transfer from the polymer matrix to the reinforcing fibers.

3.2 | Rheological Behavior of WCFF/PP Composites

Figure 3a,b shows the storage modulus (G') and complex viscosity (η^*) of PP and WCFF/PP composites, revealing the effects of WCFF incorporation, MA-g-PP addition, and sieving of WCFF. Although running rheology tests at 230°C resulted in browning of the samples, catastrophic thermal decomposition was not occurring as TGA showed peak degradation of WCFF at 355°C (Figure 8). Instead, the cellulosic component was experiencing more moderate thermal or chemical modification during the extended time under shear at this elevated temperature. Foaming and voids were not observed, confirming that 230°C was not hot enough to cause off-gassing. Furthermore, time sweeps at 200°C (data not shown) revealed less than 10% change in rheological properties of SF0-MA0 and approximately a 30% change in SF0 within 10 min, which is approximately the time needed to complete a frequency sweep test. The greater reduction observed in SF0 is attributed to the presence of MA-g-PP, rather than degradation of the WCFF.

Both G' and η^* were lower at 230°C, compared to those at 170°C for all the cases, as expected. Higher thermal energy increased polymer chain mobility, reducing entanglements and intermolecular interactions responsible for melt elasticity and flow resistance. All samples exhibited typical shear-thinning behavior on the complex viscosity plot (Figure 3 inset). Incorporating 20 wt.%

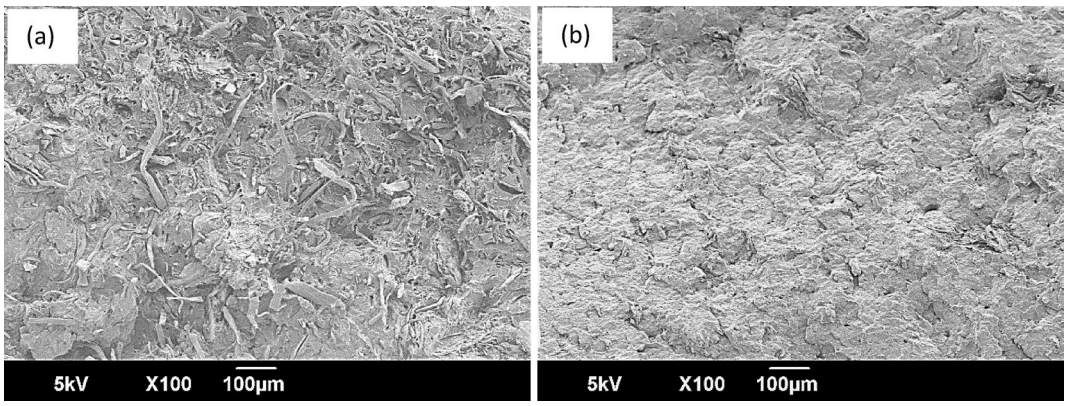

FIGURE 1 | SEM micrographs representing the morphology of the cryo-fractured samples of WCFF/PP composites (a) without MA-g-PP (SF0 sample) and (b) with 3 wt.% MA-g-PP (SF0-MA0 sample).

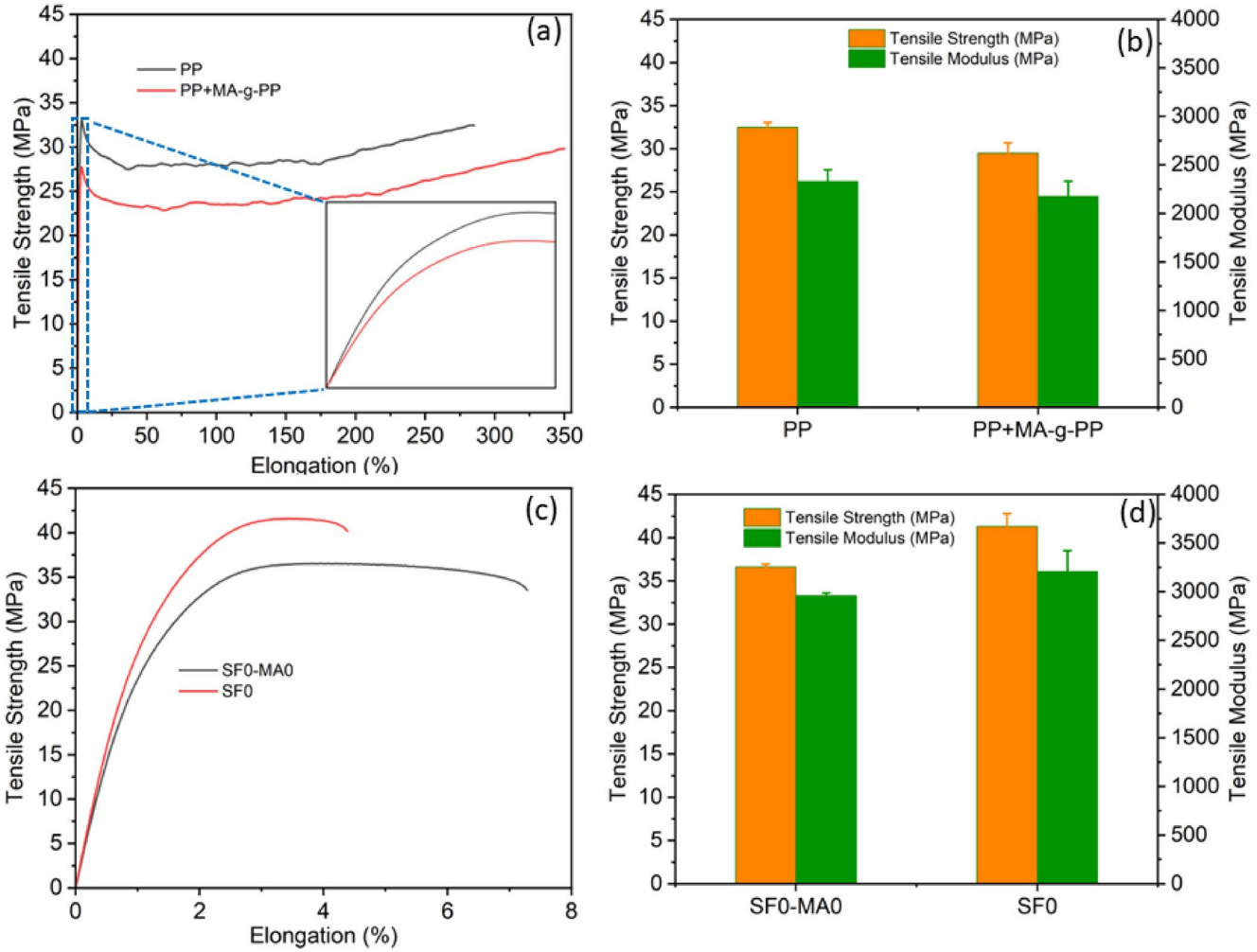

FIGURE 2 | (a) Stress versus strain curve and (b) tensile strength and modulus of the PP and PP+MA-g-PP (c) Stress versus strain curve and (d) tensile strength and modulus of the WCFF/PP composites with (SF0) and without MA-g-PP (SF0-MA0).

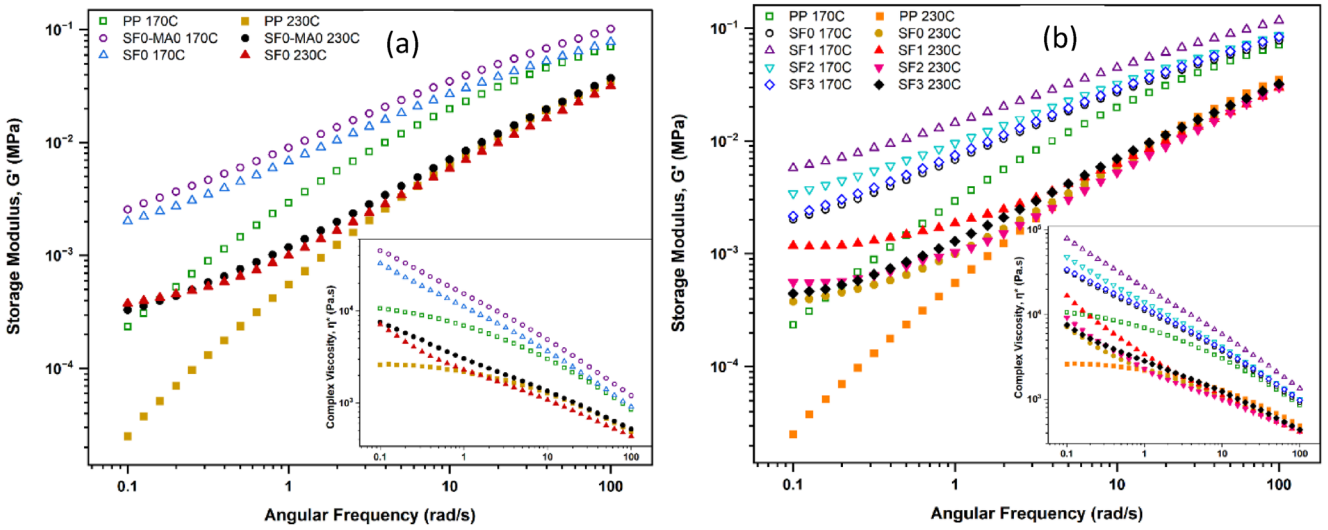

FIGURE 3 | Storage modulus and complex viscosity as a function of frequency showing (a) the effect of MA-g-PP on WCFF/PP composites at 170°C and 230°C and (b) the effect of particle size on WCFF/PP composites at 170°C and 230°C.

WCFF into PP increased G' and η^* across the frequency sweep at 170°C, compared to neat PP, with the enhancement less prominent at higher frequencies (Figure 3a). This enhancement was due to fibers restricting polymer chain flow, increasing the composite's resistance to shear stress-induced deformation [17]. The addition of MA-g-PP slightly reduced G' (at 170°C) and η^* (at both 170°C

and 230°C) of the WCFF/PP composite (Figure 3a). This reduction was attributed to a better dispersion of fibers/fines as well as improved adhesion between the PP matrix and WCFF interface, resulting in lower resistance of the composite to flow. Although not measured, we speculate that the MA-g-PP had a lower molecular weight, decreasing the effective entanglement in the melt [17–19]. At 170°C, the rheological response was reduced over all frequencies. However, at 230°C, SF0 displayed more pronounced plateauing of the G' at low frequencies, indicative of a strong network formation with the addition of MA-g-PP.

The rheological responses of the composites exhibited variations dependent on particle size. The highest storage modulus and viscosity were associated with SF1 at both temperatures (Figure 3b). SF1 possessed fibers with the largest aspect ratios (Table 1). Moving from SF1 to SF3, as the fiber aspect ratio decreases, G' and η^* decreased. These differences are particularly larger at low frequency ranges. At a given loading of filler (20 wt.% here), a larger aspect ratio provides a more effective percolative network and thus more resistance to flow. Also, the observed enhancements at lower frequency ranges can be attributed to fiber-polymer matrix interactions that cannot be altered at low frequencies [20]. Although SF0 (nonsieved) had the broadest fiber size distribution compared to other formulations, the negligible differences in rheological behavior between SF0 and SF3 at 170°C across all frequencies (Figure 3b) suggest that SF0 contained a significant proportion of SF3-sized particles. Similar observations of the aspect ratio effect have also been demonstrated in nanocomposite systems [21].

Figure 4 illustrates the MFI results for all the samples given in Table 1. The MFI value of PP, SF0-MA0, SF0, SF1, SF2, and SF3 were measured to be 2.42, 0.88, 0.88, 0.52, 0.78, and 0.84 g/10 min, respectively. The data shows a noticeable change in MFI when 20 wt.% WCFF was added to PP, consistent with the complex viscosity data. The inclusion of MA-g-PP had little impact on the flow characteristics of WCFF/PP composites. Moreover, at a constant WCFF content of 20 wt.%, an increase in the size range from SF3 to SF1 resulted in a further decrease in MFI. This trend again aligns with the complex viscosity data above. Soleimani et al. [22] and Panthapulakkal et al. [23] reported a reduction in MFI with the addition of fiber due to restriction in flow, and Huang et al. reported a reduction in MFI with fiber aspect ratio similar to the observations here [24].

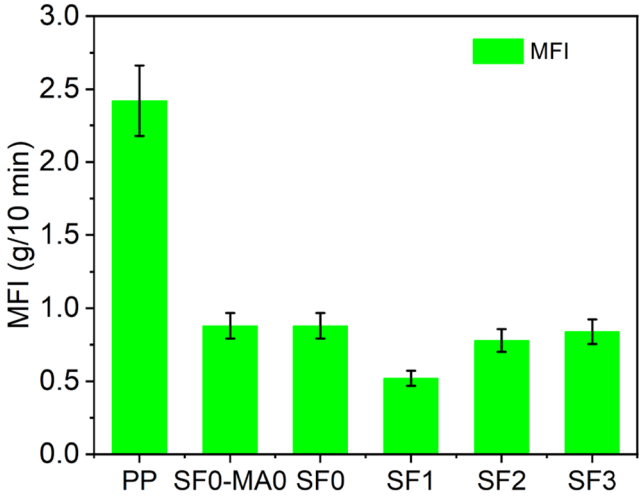

FIGURE 4 | MFI of WCFF/PP composites showing the effect of WCFF and its size on the PP's melt flow index.

3.3 | Tensile Properties of WCFF/PP Composites

Figure 5a,b show the stress versus strain plots of the pristine PP and 20 wt.% WCFF reinforced composites having different sieving mesh sizes, that is SF0, SF1, SF2, and SF3 of Table 1. Pristine PP shows a ductile behavior while all the composites went through a brittle fracture without any significant plastic deformation. PP exhibited a tensile strength of 32.45 MPa, whereas SF0, SF1, SF2, and SF3 composites showed a tensile strength of 41.28, 31.04, 28.15, and 28.18 MPa, respectively (Figure 5c). It is evident, especially for composites from SF1 to SF3, that with the decreasing mesh size, a decrease in the tensile strength was exhibited, attributed to the decreased aspect ratio of the fibers. Interestingly, the composite SF0 reported the greatest tensile strength among all the samples. It was presumed that nonsieved WCFF with a mix of both particulate and fibrous reinforcement performed as a hybrid composite. Larger fibers acted as primary reinforcement with the support of small particulates as secondary hybridizing particles. Similar results have been reported by Gogoi et al. [25] for the hollow glass microspheres (HGM) and carbon fiber reinforced PP composites. In their study, the authors found that only carbon fiber or HGM reinforced PP composites exhibited lower tensile strength values, compared to a mix of both HGM and carbon fiber reinforced PP hybrid composites. In other studies, Khandelwal et al. [26] and Sumesh et al. [27] reported that the use of nano or microparticulate fillers reduced the interfacial gap between fiber and polymeric matrix and helped in more effective transferring of the load from matrix to fiber. Hence, in the current study, composites reinforced with nonsieved reinforcement (a combination of both long cellulosic fibers and cellulose fines) having the highest tensile strength among all the composites, could have benefited from this hybridization mechanism.

As seen in Figure 5d, the tensile modulus also followed a similar trend as the strength. The modulus of SF0, SF1, SF2, and SF3 composites was measured to be 3207, 2660, 2234, and 2172 MPa, respectively (Figure 4d). The composites of SF0 and SF1 demonstrated a higher tensile modulus than that of the pristine PP (2330 MPa). Again, the combination of large fiber size and microparticles in nonsieved fibers resulted in the highest tensile modulus of the SF0 composites due to the positive hybridization effect. As shown in Figure 5e,f, the elongation at break of all the composites decreased significantly compared to the pristine PP case. No significant difference was observed between the elongation at break of different composites. The decrease in the elongation at break was attributed to the addition of the hard and stiff WCFF filler, with low deformability, which causes the composite system to be brittle with a sharp drop in the elongation at break [28]. This observation is in line with the data reported by various researchers, where the addition of hard and stiff fiber led to a sharp drop in elongation at break and impact properties of the composites, as summarized in this review article [29]. Furthermore, the presence of MA-g-PP also caused a drop in the elongation at break (Figure 2a), due to its additional stiffening effect through enhanced interface. It has been reported that during crack propagation, fibers need to break or pull out

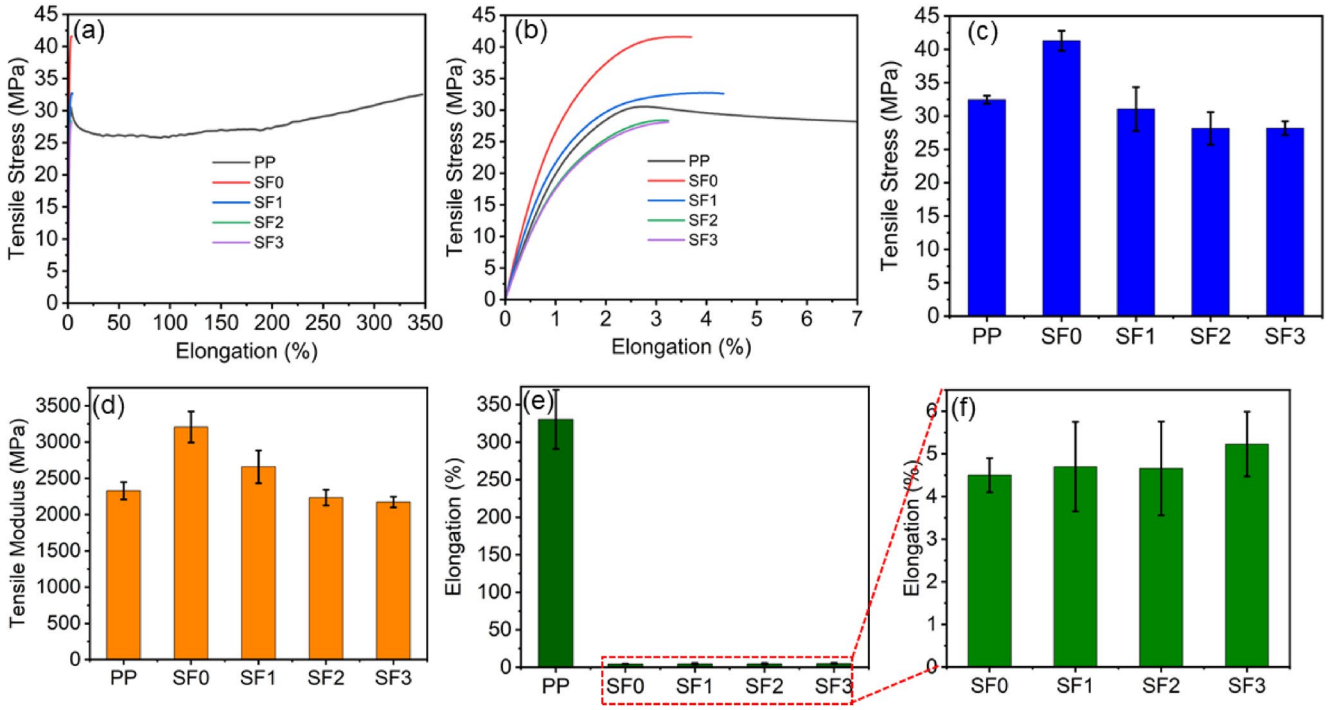

FIGURE 5 | Effect of different fiber sizes on the tensile properties (a, b) tensile stress versus elongation (c) tensile stress (d) tensile modulus (e, f) elongation at break.

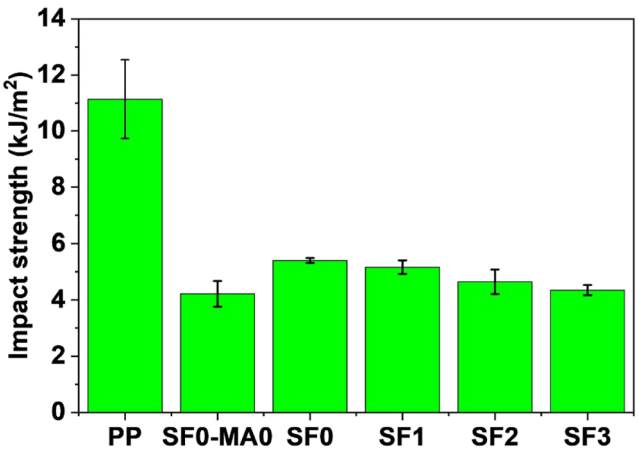

FIGURE 6 | Effect of different fiber sizes on Izod notched impact strength of PP composite.

of the matrix. However, the presence of a compatibilizer increases the chance of fiber breakage due to the strong interfacial adhesion, leading to lower elongation at break [30]. The above results and discussion confirm that nonsieved fibers outperformed all the sieved fibers and improved the strength and modulus of the pristine PP by 24.2% and 37.7%, respectively. These findings suggest that a sieving process may not be necessary for the utilization of waste cellulosic feedstocks.

Figure 6 shows the impact strength of the pristine PP and 20 wt.% WCFF loaded composites with different sieving mesh sizes, namely SF0, SF1, SF2, and SF3 as listed in Table 1. Pristine PP exhibits ductile behavior with an impact strength of 11.14 kJ/m^2, whereas all the composites display lower impact strengths. The impact strengths of SF0-MA0, SF0, SF1, SF2, and SF3 were 4.22, 5.41, 5.17, 4.64, and 4.35 kJ/m^2, respectively. Similar results have been reported by Bengtsson et al. [31], where the impact strength of the cellulose fiber reinforced PP composites was significantly lower than that of the neat PP. As reported, stiffer cellulose fibers and their interfaces with the matrix can act as stress concentrators in the composite, thus reducing the material resistance to crack initiation and growth and consequently reducing the impact strength [31–33]. Moreover, the SF0 composite showed higher impact strength than SF0-MA0 because of the addition of the compatibilizer, as also reported in Ashori et al. [34] More interestingly, the composite samples SF1 to SF3 showed a reduction in the impact strength as the WCFF mesh size decreased. Although there is no study directly analyzing the mesh size effect of WCFF, past works have shown that the impact strength decreases with a reduction in the fiber aspect ratio [35, 36].

3.4 | Thermal Properties of WCFF/PP Composites

Figure 7a,b show the cooling and second heating thermograms of the pristine PP and WCFF/PP composites, respectively. Likewise, Figure 7c shows the peak crystallization temperature (T_c) and crystallinity (X), calculated from the second heating thermograms. SF0, SF1, SF2, and SF3 showed a T_c of 121.1°C, 121.0°C, 121.4°C, and 120.8°C, respectively, which all were lower than the T_c of the pristine PP (128.7°C). A similar result has been reported for the sunflower hull sanding dust-reinforced composites by Sui et al. [16]. Moreover, no significant difference was observed between the T_c values of various WCFF/PP composite. In other words, at a given WCFF loading (20 wt.%), the sieving size did not appear to significantly affect the T_c of the composites. In addition, the T_m of PP did not change significantly due to the addition of WCFF. However, as seen in Figure 7c, overall,

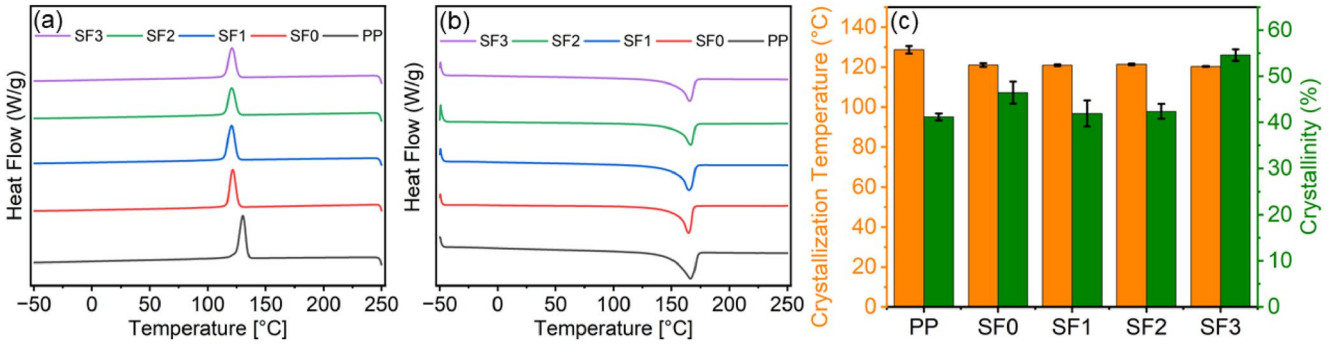

FIGURE 7 | (a) Cooling thermograms, (b) second heating thermograms, and (c) crystallization temperature (T_c) and crystallinity (X) of WCFF/PP composites.

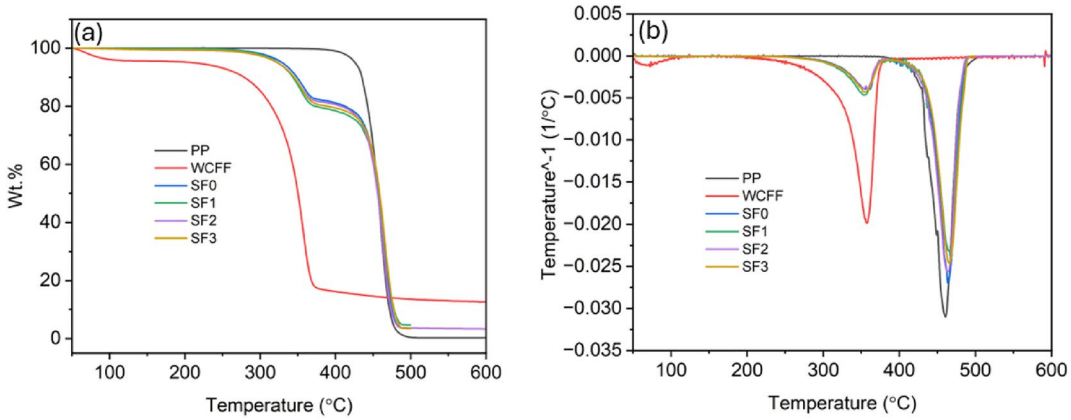

FIGURE 8 | (a) Weight percentage and (b) temperature derivative weight loss as a function of temperature for PP, WCFF, and WCFF/PP composites.

PP's crystallinity was increased after the addition of WCFF, but the level of improvement was dependent on the sieving size. The composite SF3, reinforced with the smallest WCFF mesh size (lower than 0.82 mm) exhibited the highest crystallinity of 54.6%, indicating a 32.6% increase, compared to that of pristine PP. The second largest increase in crystallinity was for SF0 case (13.0%). The composites having fibers with large aspect ratio, that is SF1 and SF2 demonstrated crystallinity values only slightly larger than that of PP.

Although fillers can potentially act as a crystal nucleating agent, Sui et al. [16] have reported that fillers were found to also obstruct the mobilization of the PP macromolecular chain and prevent the macromolecular segment from obtaining ordered alignment in the crystal lattice. Therefore, overall, the crystallization temperature and crystallinity of a two-phase or three-phase composite depend on the competition between heterogeneous nucleation provided by the reinforcements and the obstructions created by them during the crystal formation of the matrix. The composite SF3 had the smallest size of cellulose fillers, and it appears that small-sized fillers provided a better opportunity for crystal nucleation, whereas their obstruction effect during chain stacking may not have been as severe due to their smaller size. Thus, it provided the highest crystallinity. Similarly, SF0, which is the nonsieved case, did include a substantial fraction of small-sized fillers, providing the second most increase in the crystallinity. The effect of filler size on polymer chain mobility can also be inferred from the rheological observations, where SF1 and SF2 exhibited higher viscosity values compared to those of SF0 and SF3 (Figure 3b). In a similar study, the effect of fiber length on the crystallinity of the glass fiber-reinforced PP composites was investigated by Seong et al. [37]. The authors reported that the composites reinforced with 2 mm fiber length demonstrated higher crystallinity ($X = 55.9\%$), compared to those reinforced with 10 mm fiber size ($X = 52.9\%$).

The thermal stability and degradation behavior of PP, WCFF, and WCFF/PP composites were studied using thermogravimetric analysis and the results are gathered in Figure 8. Pristine PP and WCFF underwent single-step degradation, whereas WCFF/PP composites followed a two-step degradation (Figure 8a) [38, 39]. Pristine WCFF showed an initial weight loss of about 5%, which could be due to the moisture removal. In Figure 8b, the mass loss peaked at around 355°C, which was associated with the degradation of cellulose, and the other one peaked at around 460°C, which was for PP degradation [40]. In WCFF/PP composites, the peak temperatures of WCFF and PP components remained approximately unchanged. However, the onset temperature of WCFF in the composites increased from around 220°C for the pristine WCFF to 282°C, indicating an improved stability of cellulose once integrated in the PP matrix. The onset temperature was the same for all the composites, as they all included the same amount of WCFF (20 wt.%) [41] and the filler size did not seem to have any effect. It has been reported that the onset temperature decreases with increasing fiber content [40]. At the end of the TGA experiment, pristine PP and WCFF left a residue of 0.3% and 12.0%, respectively, and the residue of the composites was about 3–4 wt.%.

With the widespread development of plant-based fiber reinforced polymer composite, this work sheds some light on the suitability of incorporating waste plant base materials as reinforcing agents in polymer composites. Many literature works have reported that natural fiber-reinforced composites can be successfully used for the fabrication of automotive components, such as door panels, racing car seats, inserts, rear parcel shelves, seat backs, spare tire covers, and interior trims. For instance, Pradeep et al. reported the properties and use of various polymeric composites for door panels used by various automakers [42]. In their investigation, the authors found that Audi, Daimler Chrysler, and Dodge reported a tensile strength of 40–50, 30–60, and 15–26 MPa for door panel applications using flax/sisal/polyurethane rubber, flax/hemp/coconut/PP, and TPO [42]. Interestingly, the tensile strength of the composites fabricated from WCFF and PP in this work falls in the same range.

4 | Conclusions

WCFF mixture from the paper industry was received in large pellet form and dissociated into a feedable fibrous form using a gentle grinding process. The down-sized WCFF was sieved using different mesh sizes and compounded with PP with and without MA-g-PP. The compounding was conducted using a twin-screw extruder, followed by sample preparation using compression molding. The morphological analysis confirmed that the incorporation of MA-g-PP in the composites enhanced the dispersion of WCFF increased the cellulose/PP interfacial adhesion. Incorporating 20 wt.% WCFF into PP increased the storage modulus (G') and complex viscosity (η^*) of the composites at 170°C. The rheological tests at the extreme temperature of 230°C revealed a reduction in both G' and η^*, due to an increased polymer chain mobility, as expected. The browning observed at 230°C indicated some level of thermal or chemical modification during rheological testing, highlighting differences between dynamic rheological testing and TGA measurements. Moreover, the maximum increase in G' and η^* was observed for the samples loaded with nonsieved WCFF (SF0), due to a larger fiber aspect ratio and synergistic effect of fibers and fines. In addition, the MFI measurements also revealed that the melt flowability slightly decreased with an increase in the WCFF mesh size. The highest tensile strength and modulus were found for the composite fabricated using nonsieved WCFF, offering 28% and 38% enhancements, respectively, over pristine PP. The outperformance of nonsieved WCFF, compared to the sieved fibers, was attributed to the positive hybridization effect of a mixture of large aspect ratio (fiber) and small aspect ratio (fine) fillers. However, the impact strength of the PP/WCFF composites was lower than that of the pristine PP. Overall, the tensile strength, tensile modulus and impact strength all increased as the mesh size was increased, which could be due to the inclusion of a greater number of large-aspect-ratio fillers.

Thermal analysis showed that overall, the PP's crystallization temperature decreased by the introduction of 20 wt.% WCFF and 3 wt.% MA-g-PP to pristine PP. The PP's crystallinity, however, exhibited a relatively strong dependency on the sieving, where WCFF samples having a larger number of finer fillers promoted the crystallinity significantly, whereas others with large-aspect-ratio fillers had minimal impact on crystallinity. Moreover, it was found that the WCFF degradation onset temperature increased significantly once it was incorporated into the PP matrix, offering melt processability benefits. This study suggests that waste cellulosic mixtures may be utilized as effective reinforcement without any additional sieving and separation to manufacture high-performance and cost-effective polymer composites.

Author Contributions

Conceptualization: Davide Masato, Margaret J. Sobkowicz, and Amir Ameli. Data curation: Emmanuel Akubueze, Atul Kumar Maurya, Patrick Masembe, Niyi Olaiya, and Nicholas Bowen. Formal analysis: Emmanuel Akubueze, Atul Kumar Maurya, Patrick Masembe, Niyi Olaiya, and Nicholas Bowen. Funding acquisition: Davide Masato, Margaret J. Sobkowicz, and Amir Ameli. Investigation: Atul Kumar Maurya, Niyi Olaiya, Davide Masato, Margaret J. Sobkowicz, and Amir Ameli. Methodology: Atul Kumar Maurya, Niyi Olaiya, Davide Masato, Margaret J. Sobkowicz, and Amir Ameli. Project administration: Amir Ameli. Resources: Davide Masato, Margaret J. Sobkowicz, and Amir Ameli. Supervision: Davide Masato, Margaret J. Sobkowicz, and Amir Ameli. Validation: Davide Masato, Margaret J. Sobkowicz, and Amir Ameli. Visualization: Emmanuel Akubueze, Atul Kumar Maurya, Patrick Masembe, Niyi Olaiya, and Nicholas Bowen. Writing – original draft: Emmanuel Akubueze, Atul Kumar Maurya, and Niyi Olaiya. Writing – review and editing: Patrick Masembe, Niyi Olaiya, Nicholas Bowen, Davide Masato, Margaret J. Sobkowicz, and Amir Ameli.

Acknowledgments

This material is based upon work supported by the U.S. Department of Energy's Office of Energy Efficiency and Renewable Energy (EERE) under the Advanced Manufacturing Office Award Number DE-EE0007897. This paper was prepared from results obtained as part of the project sponsored by an agency of the United States Government. Neither the United States Government nor any agency thereof, nor any of their employees, makes any warranty, express or implied, or assumes any legal liability or responsibility for the accuracy, completeness, or usefulness of any information, apparatus, product, or process disclosed, or represents that its use would not infringe privately owned rights. Reference herein to any specific commercial product, process, or service by trade name, trademark, manufacturer, or otherwise does not necessarily constitute or imply its endorsement, recommendation, or favoring by the United States Government or any agency thereof. The views and opinions of authors expressed herein do not necessarily state or reflect those of the United States Government or any agency thereof. The authors also would like to thank American Wood Fibers for supplying the waste cellulosic materials. We also thank Dr. Zhihua Jiang for size analysis of waste cellulosic materials.

Conflicts of Interest

The authors declare no conflicts of interest.

Data Availability Statement

The data that support the findings of this study are available from the corresponding author upon reasonable request.

References

1. M. K. Lila, A. Singhal, S. S. Banwait, and I. Singh, "A Recyclability Study of Bagasse Fiber Reinforced Polypropylene Composites," *Polymer Degradation and Stability* 152 (2018): 272–279.

2. A. K. Maurya, R. Gogoi, and G. Manik, "Recycling and Reinforcement Potential for the Fly Ash and Sisal Fiber Reinforced Hybrid Polypropylene Composite," *Polymer Composites* 43 (2022): 1060–1077.

3. S. Ramarad, M. Khalid, C. T. Ratnam, A. L. Chuah, and W. Rashmi, "Waste Tire Rubber in Polymer Blends: A Review on the Evolution, Properties and Future," *Progress in Materials Science* 72 (2015): 100–140.

4. J. Kumar, A. K. Maurya, H. S. Gupta, S. P. Singh, and C. Sharma, "Development of Eco-Friendly Bio-Composite by Reinforcing Pineapple Fruit Waste Crown Fiber to Ethylene-Propylene Rubber Modified Polyethylene," *Polymer Composites* 43 (2022): 8259–8273.

5. S. Chandra Dubey, V. Mishra, and A. Sharma, "A Review on Polymer Composite With Waste Material as Reinforcement," *Materials Today Proceedings* 47 (2021): 2846–2851.

6. A. K. Maurya and G. Manik, "Development and Characterization of a Recycled Nylon Fiber Reinforced and Nano-Fly Ash Hybridized High Impact Performance Polypropylene Composite for Sustainability," *Journal of Thermoplastic Composite Materials* 36, no. 10 (2022): 4042, https://doi.org/10.1177/08927057221147825.

7. A. K. Maurya and G. Manik, "Advances Towards Development of Industrially Relevant Short Natural Fiber Reinforced and Hybridized Polypropylene Composites for Various Industrial Applications: A Review," *Journal of Polymer Research 2022* 30, no. 1 (2023): 47.

8. N. M. Nurazzi, M. M. Harussani, H. A. Aisyah, et al., "Treatments of Natural Fiber as Reinforcement in Polymer Composites—A Short Review," *Functional Composites and Structures* 3 (2021): 024002.

9. F. E. El-Abbassi, M. Assarar, R. Ayad, et al., "Effect of Alkali Treatment on Alfa Fibre as Reinforcement for Polypropylene Based Eco-Composites: Mechanical Behaviour and Water Ageing," *Composite Structures* 133 (2015): 451–457.

10. J. Z. Lu, A. Professor, H. S. McNabb, et al., "Chemical Coupling in Wood Fiber and Polymer Composites: A Review of Coupling Agents and Treatments," *Wood and Fiber Science* 32, no. 1 (2000): 88–104.

11. R. Gogoi, N. Kumar, S. Mireja, S. S. Ravindranath, G. Manik, and S. Sinha, "Effect of Hollow Glass Microspheres on the Morphology, Rheology and Crystallinity of Short Bamboo Fiber-Reinforced Hybrid Polypropylene Composite," *JOM* 71 (2019): 548–558.

12. A. K. Maurya, R. Gogoi, and G. Manik, "Sisal Fiber/Fly Ash-Reinforced Hybrid Polypropylene Composite: An Investigation Into the Thermal, Rheological, and Crystallographic Properties," in *Lecture Notes in Mechanical Engineering* (Springer Nature Singapore, 2023), 721–731.

13. B. Wang, F. H. Lin, X. Li, et al., "Isothermal Crystallization and Rheology Properties of Isotactic Polypropylene/Bacterial Cellulose Composite," *Polymers* 10 (2018): 1284.

14. O. A. Ogah, "Rheological Properties of Natural Fiber Polymer Composites," *MOJ Polymer Science* 1 (2017): 1, https://doi.org/10.15406/MOJPS.2017.01.00022.

15. S. J. Kim, J. B. Moon, G. H. Kim, and C. S. Ha, "Mechanical Properties of Polypropylene/Natural Fiber Composites: Comparison of Wood Fiber and Cotton Fiber," *Polymer Testing* 27 (2008): 801–806.

16. G. Sui, M. A. Fuqua, C. A. Ulven, and W. H. Zhong, "A Plant Fiber Reinforced Polymer Composite Prepared by a Twin-Screw Extruder," *Bioresource Technology* 100 (2009): 1246–1251.

17. H. L. Tekinalp, D. Ker, X. Zhao, et al., "Effect of Surface Treatment of Microfiberlated Cellulose Fibers on Biocomposite Properties and Additive Manufacturing Process," CAMX 2019—Composites and Advanced Materials Expo, https://doi.org/10.33599/NASAMPE/C.19.0772.

18. Y. C. Kim, S. J. Lee, J. C. Kim, et al., "Effect of Maleated Polyethylene on the Rheological Properties of LLDPE/Clay Nanocomposites," *Polymer Journal* 37 (2005): 206–213.

19. N. Inul Azianti and A. Ishak, "Effect of Fiber Loading and Compatibilizer on Rheological, Mechanical and Morphological Behaviors," *Open Journal of Polymer Chemistry* 2012 (2012): 31–41.

20. R. Cherizol, M. Sain, and J. Tjong, "Evaluation of the Influence of Fibre Aspect Ratio and Fibre Content on the Rheological Characteristic of High Yield Pulp Fibre Reinforced Polyamide 11 "HYP/PA11" Green Composite," *Open Journal of Polymer Chemistry* 05 (2015): 1–8.

21. G. Bernagozzi, D. Battegazzore, R. Arrigo, and A. Frache, "Optimizing the Rheological and Thermal Behavior of Polypropylene-Based Composites for Material Extrusion Additive Manufacturing Processes," *Polymers (Basel)* 15 (2023): 2263.

22. M. Soleimani, L. Tabil, S. Panigrahi, and A. Opoku, "The Effect of Fiber Pretreatment and Compatibilizer on Mechanical and Physical Properties of Flax Fiber-Polypropylene Composites," *Journal of Polymers and the Environment* 16 (2008): 74–82.

23. S. Panthapulakkal, M. Sain, and S. Law, "Effect of Coupling Agents on Rice-Husk-Filled HDPE Extruded Profiles," *Polymer International* 54 (2005): 137–142.

24. P. W. Huang, H. S. Peng, S. J. Hwang, and C. T. Huang, "The Low Breaking Fiber Mechanism and Its Effect on the Behavior of the Melt Flow of Injection Molded Ultra-Long Glass Fiber Reinforced Polypropylene Composites," *Polymers (Basel)* 13 (2021): 2492.

25. R. Gogoi, G. Manik, and B. Arun, "High Specific Strength Hybrid Polypropylene Composites Using Carbon Fibre and Hollow Glass Microspheres: Development, Characterization and Comparison With Empirical Models," *Composites Part B, Engineering* 173 (2019): 106875.

26. S. Khandelwal and K. Y. Rhee, "Recent Advances in Basalt-Fiber-Reinforced Composites: Tailoring the Fiber-Matrix Interface," *Composites Part B: Engineering* 192 (2020): 108011.

27. K. R. Sumesh, V. Kavimani, G. Rajeshkumar, P. Ravikumar, and S. Indran, "An Investigation Into the Mechanical and Wear Characteristics of Hybrid Composites: Influence of Different Types and Content of Biodegradable Reinforcements," *Journal of Natural Fibers* 19 (2022): 2823–2835.

28. T. Quynh Truong Hoang, F. Lagattu, and J. Brillaud, "Natural Fiber-Reinforced Recycled Polypropylene: Microstructural and Mechanical Properties," *Journal of Reinforced Plastics and Composites* 29 (2008): 209–217.

29. A. Nourbakhsh, B. V. Kokta, A. Ashori, and A. Jahan-Latibari, "Effect of a Novel Coupling Agent, Polybutadiene Isocyanate, on Mechanical Properties of Wood-Fiber Polypropylene Composites," *Journal of Reinforced Plastics and Composites* 27 (2008): 1679–1687.

30. M. Mihalic, L. Sobczak, C. Pretschuh, et al., "Increasing the Impact Toughness of Cellulose Fiber Reinforced Polypropylene Composites—Influence of Different Impact Modifiers and Production Scales," *Journal of Composites Science* 3 (2019): 82.

31. M. Bengtsson, M. Le Baillif, and K. Oksman, "Extrusion and Mechanical Properties of Highly Filled Cellulose Fibre–Polypropylene Composites," *Composites Part A, Applied Science and Manufacturing* 38 (2007): 1922–1931.

32. A. L. Catto, M. A. Dahlem Júnior, B. Hansen, E. L. Francisquetti, and C. Borsoi, "Characterization of Polypropylene Composites Using Yerba Mate Fibers as Reinforcing Filler," *Composites Part B: Engineering* 174 (2019): 106935.

33. S. Kaewkuk, W. Sutapun, and K. Jarukumjorn, "Effects of Interfacial Modification and Fiber Content on Physical Properties of Sisal Fiber/Polypropylene Composites," *Composites Part B: Engineering* 45 (2013): 544–549.

34. A. Ashori and A. Nourbakhsh, "Performance Properties of Microcrystalline Cellulose as a Reinforcing Agent in Wood Plastic Composites," *Composites Part B: Engineering* 41 (2010): 578–581.

35. R. Gu and B. V. Kokta, "Mechanical Properties of Pp Composites Reinforced With BCTMP Aspen Fiber," *Journal of Thermoplastic Composite Materials* 23 (2010): 513–542.

36. A. M. Seid and S. A. Adimass, "Review on the Impact Behavior of Natural Fiber Epoxy Based Composites," *Heliyon* 10 (2024): e39116.

37. D. G. Seong, C. Kang, S. Y. Pak, C. H. Kim, and Y. S. Song, "Influence of Fiber Length and Its Distribution in Three Phase Poly(Propylene) Composites," *Composites Part B: Engineering* 168 (2019): 218–225.

38. N. M. Nurazzi, M. R. M. Asyraf, M. Rayung, et al., "Thermogravimetric Analysis Properties of Cellulosic Natural Fiber Polymer Composites: A Review on Influence of Chemical Treatments," *Polymers* 13, no. 16 (2021): 2710.

39. M. Tajvidi and A. Takemura, "Thermal Degradation of Natural Fiber-Reinforced Polypropylene Composites," *Journal of Thermoplastic Composite Materials* 23, no. 3 (2009): 281–298.

40. A. K. Maurya, R. Gogoi, and G. Manik, "Thermal Behavior of Elastomer Blends and Composites," in *Elastomer Blends and Composites: Principles, Characterization, Advances, and Applications* (Elsevier, 2022), 149–169.

41. A. K. Maurya, R. Gogoi, and G. Manik, "Mechano-Chemically Activated Fly-Ash and Sisal Fiber Reinforced PP Hybrid Composite With Enhanced Mechanical Properties," *Cellulose* 28 (2021): 8493–8508.

42. S. A. Pradeep, R. K. Iyer, H. Kazan, et al., "Automotive Applications of Plastics: Past, Present, and Future," in *Applied Plastics Engineering Handbook: Processing, Materials, and Applications*, 2nd ed. (William Andrew Publishing, 2017), 651–673.